

Measurement of $\mathcal{B}(D^+ \rightarrow \bar{K}^{*0} l^+ \nu_l)$

G. Brandenburg,¹ A. Ershov,¹ D. Y.-J. Kim,¹ R. Wilson,¹ K. Benslama,² B. I. Eisenstein,² J. Ernst,² G. D. Gollin,² R. M. Hans,² I. Karliner,² N. Lowrey,² M. A. Marsh,² C. Plager,² C. Sedlack,² M. Selen,² J. J. Thaler,² J. Williams,² K. W. Edwards,³ R. Ammar,⁴ D. Besson,⁴ X. Zhao,⁴ S. Anderson,⁵ V. V. Frolov,⁵ Y. Kubota,⁵ S. J. Lee,⁵ S. Z. Li,⁵ R. Poling,⁵ A. Smith,⁵ C. J. Stepaniak,⁵ J. Urheim,⁵ S. Ahmed,⁶ M. S. Alam,⁶ L. Jian,⁶ M. Saleem,⁶ F. Wappler,⁶ E. Eckhart,⁷ K. K. Gan,⁷ C. Gwon,⁷ T. Hart,⁷ K. Honscheid,⁷ D. Hufnagel,⁷ H. Kagan,⁷ R. Kass,⁷ T. K. Pedlar,⁷ J. B. Thayer,⁷ E. von Toerne,⁷ T. Wilksen,⁷ M. M. Zoeller,⁷ S. J. Richichi,⁸ H. Severini,⁸ P. Skubic,⁸ S. A. Dytman,⁹ S. Nam,⁹ V. Savinov,⁹ S. Chen,¹⁰ J. W. Hinson,¹⁰ J. Lee,¹⁰ D. H. Miller,¹⁰ V. Pavlunin,¹⁰ E. I. Shibata,¹⁰ I. P. J. Shipsey,¹⁰ D. Cronin-Hennessy,¹¹ A. L. Lyon,¹¹ C. S. Park,¹¹ W. Park,¹¹ E. H. Thorndike,¹¹ T. E. Coan,¹² Y. S. Gao,¹² F. Liu,¹² Y. Maravin,¹² I. Narsky,¹² R. Stroynowski,¹² J. Ye,¹² M. Artuso,¹³ C. Boulahouache,¹³ K. Bukin,¹³ E. Dambasuren,¹³ R. Mountain,¹³ T. Skwarnicki,¹³ S. Stone,¹³ J. C. Wang,¹³ A. H. Mahmood,¹⁴ S. E. Csorna,¹⁵ I. Danko,¹⁵ Z. Xu,¹⁵ G. Bonvicini,¹⁶ D. Cinabro,¹⁶ M. Dubrovin,¹⁶ S. McGee,¹⁶ A. Bornheim,¹⁷ E. Lipeles,¹⁷ S. P. Pappas,¹⁷ A. Shapiro,¹⁷ W. M. Sun,¹⁷ A. J. Weinstein,¹⁷ G. Masek,¹⁸ H. P. Paar,¹⁸ R. Mahapatra,¹⁹ R. A. Briere,²⁰ G. P. Chen,²⁰ T. Ferguson,²⁰ G. Tatishvili,²⁰ H. Vogel,²⁰ N. E. Adam,²¹ J. P. Alexander,²¹ C. Bebek,²¹ K. Berkelman,²¹ F. Blanc,²¹ V. Boisvert,²¹ D. G. Cassel,²¹ P. S. Drell,²¹ J. E. Duboscq,²¹ K. M. Ecklund,²¹ R. Ehrlich,²¹ L. Gibbons,²¹ B. Gittelman,²¹ S. W. Gray,²¹ D. L. Hartill,²¹ B. K. Heltsley,²¹ L. Hsu,²¹ C. D. Jones,²¹ J. Kandaswamy,²¹ D. L. Kreinick,²¹ A. Magerkurth,²¹ H. Mahlke-Krüger,²¹ T. O. Meyer,²¹ N. B. Mistry,²¹ E. Nordberg,²¹ M. Palmer,²¹ J. R. Patterson,²¹ D. Peterson,²¹ J. Pivarski,²¹ D. Riley,²¹ A. J. Sadoff,²¹ H. Schwarthoff,²¹ M. R. Shepherd,²¹ J. G. Thayer,²¹ D. Urner,²¹ B. Valant-Spaight,²¹ G. Viehhauser,²¹ A. Warburton,²¹ M. Weinberger,²¹ S. B. Athar,²² P. Avery,²² H. Stoeck,²² and J. Yelton²²

(CLEO Collaboration)

¹Harvard University, Cambridge, Massachusetts 02138

²University of Illinois, Urbana-Champaign, Illinois 61801

³Carleton University, Ottawa, Ontario, Canada K1S 5B6
and the Institute of Particle Physics, Canada M5S 1A7

⁴University of Kansas, Lawrence, Kansas 66045

⁵University of Minnesota, Minneapolis, Minnesota 55455

⁶State University of New York at Albany, Albany, New York 12222

⁷Ohio State University, Columbus, Ohio 43210

⁸University of Oklahoma, Norman, Oklahoma 73019

⁹University of Pittsburgh, Pittsburgh, Pennsylvania 15260

¹⁰Purdue University, West Lafayette, Indiana 47907

¹¹University of Rochester, Rochester, New York 14627

¹²Southern Methodist University, Dallas, Texas 75275

¹³Syracuse University, Syracuse, New York 13244

¹⁴University of Texas–Pan American, Edinburg, Texas 78539

¹⁵Vanderbilt University, Nashville, Tennessee 37235

¹⁶Wayne State University, Detroit, Michigan 48202

¹⁷California Institute of Technology, Pasadena, California 91125

¹⁸University of California–San Diego, La Jolla, California 92093

¹⁹University of California, Santa Barbara, California 93106

²⁰Carnegie Mellon University, Pittsburgh, Pennsylvania 15213

²¹Cornell University, Ithaca, New York 14853

²²University of Florida, Gainesville, Florida 32611

(Received 12 March 2002; published 11 November 2002)

Using 13.53 fb⁻¹ of CLEO data, we have measured the ratios of the branching fractions R_e^+ , R_μ^+ and the combined branching fraction ratio R_l^+ , defined by $R_l^+ = [\mathcal{B}(D^+ \rightarrow \bar{K}^{*0} l^+ \nu_l)] / [\mathcal{B}(D^+ \rightarrow K^- \pi^+ \pi^+)]$. We find $R_e^+ = 0.74 \pm 0.04 \pm 0.05$, $R_\mu^+ = 0.72 \pm 0.10 \pm 0.05$, and $R_l^+ = 0.74 \pm 0.04 \pm 0.05$, where the first and second errors are statistical and systematic, respectively. The known branching fraction $\mathcal{B}(D^+ \rightarrow K^- \pi^+ \pi^+)$ leads to $\mathcal{B}(D^+ \rightarrow \bar{K}^{*0} e^+ \nu_e) = (6.7 \pm 0.4 \pm 0.5 \pm 0.4)\%$, $\mathcal{B}(D^+ \rightarrow \bar{K}^{*0} \mu^+ \nu_\mu) = (6.5 \pm 0.9 \pm 0.5 \pm 0.4)\%$, and $\mathcal{B}(D^+ \rightarrow \bar{K}^{*0} l^+ \nu_l) = (6.7 \pm 0.4 \pm 0.5 \pm 0.4)\%$, where the third error is due to the uncertainty in $\mathcal{B}(D^+ \rightarrow K^- \pi^+ \pi^+)$.

The transition amplitude of the semileptonic decay $D^+ \rightarrow \bar{K}^{*0} l^+ \nu_l$ is proportional to the product of the leptonic and hadronic currents. The hadronic current is parametrized by three analytic functions called form factors, $A_1(q^2)$, $A_2(q^2)$, and $V(q^2)$ [1], where q^2 is the invariant mass squared of the virtual W boson. The form factors cannot be easily computed in quantum chromodynamics (QCD) since they are affected by significant nonperturbative contributions. Precise experimental measurements are needed to guide theoretical progress in this area. Measurements of these form factors are also valuable since, using heavy quark effective theory [2–4], they can be related to the form factors for an important decay $b \rightarrow ul\nu$, where like $D^+ \rightarrow \bar{K}^{*0} l^+ \nu_l$ the initial to final state transition takes place from a heavy to a light quark. This will lead to reduced theoretical uncertainties on the value of V_{ub} extracted from experimental studies of that decay.

In this work, the ratio of the branching fraction of $D^+ \rightarrow \bar{K}^{*0} l^+ \nu_l$ to that of $D^+ \rightarrow K^- \pi^+ \pi^+$ (R_l^+) was measured, where l stands for either an electron or a muon. In other experiments [5], the form factor ratios $r_2 = A_2/A_1$ and $r_V = V/A_1$ of $D^+ \rightarrow \bar{K}^{*0} l^+ \nu_l$ were obtained from angular correlations between the daughter particles. Combining these, we can calculate the form factors A_1 , A_2 , and V .

The data used in this study were collected with the two configurations of the CLEO detector [6] at the Cornell Electron Storage Ring (CESR). The data consist of 9.13 fb^{-1} of integrated luminosity on the $Y(4S)$ resonance and 4.40 fb^{-1} below the $B\bar{B}$ threshold. The investigated decay chain for this analysis was $D^{*+} \rightarrow D^+ \pi^0$, $D^+ \rightarrow \bar{K}^{*0} l^+ \nu$, and $\bar{K}^{*0} \rightarrow K^- \pi^+$. The use of the mass difference between D^{*+} and D^+ candidates reduced the background. This analysis assumes that the thrust axis [7] of the event approximates the direction of the D meson, as will be explained below. This approach does not work well for isotropic events. Thus, events whose ratio of the second and zeroth Fox-Wolfram moments [8] was less than or equal to 0.2 were rejected. To select electron candidates, we looked for tracks consistent with the electron hypothesis using a joint likelihood [9] formed from measurements of the specific ionization in the drift chamber and the shower energy and shape in the electromagnetic calorimeter. Muon candidates were required to penetrate at least five interaction lengths in our muon detector. To select good π^0 , all $\gamma\gamma$ pairs among γ satisfying the energy criteria in Table I for which $|M_{\gamma\gamma} - M_{\pi^0}| < 2.5\sigma$ were accepted, where σ is the standard deviation of the π^0 mass measurement, obtained as a function of π^0 mass and momentum using clean π^0 data samples. The typical value of σ is about $5 \text{ MeV}/c^2$. The four momenta of π^0 candidates were obtained from a π^0 mass-constrained fit for these selected $\gamma\gamma$ pairs. We used

all good π^0 candidates in each event. For signal events, often there were additional π^0 candidates besides the correct π^0 when one of the two correct photons was combined with other random photons. Due mainly to this, we had on the average 1.25 D^\pm decay candidates in a signal event, which fell in the signal region. Other kinematic criteria chosen to optimize our sensitivity are given in Table I. A detailed discussion for other event selection criteria such as the charged track particle identification is available elsewhere [9].

To reconstruct the momentum of the ν , two methods were used to obtain up to three values of \vec{p}_ν . In the first method, one or two values for the ν momentum were obtained assuming that the thrust direction of the event represents the D direction. Given $\vec{p}_{K\pi l}$, the constraint that $m_{K\pi l \nu} = m_{D^+}$ provided an ellipsoid of allowed D momenta. We then took the two intersections between the ellipsoid and the direction of the D . When there was no intersection, the point on the ellipsoid that lay closest to the D direction was used. The values for the ν momentum were then the difference between these D momenta and $\vec{p}_{K\pi l}$. The second method used the missing momentum of each event as an estimate of the ν momentum. If the missing momentum gave a value of $m_{K\pi l \nu}$ much greater than the mass of the D^+ (we used $m_{D^{*+}}$ for this limit), then the ν momentum estimate from the second method was discarded. Among these three ν momentum estimates, the one that gave the value of $\delta m = m_{K\pi l \nu \pi^0} - m_{K\pi l \nu}$ closest to the known value of $m_{D^{*+}} - m_{D^+}$ [10] was chosen. According to our simulation, this selection method gave the ν momentum closest to the generated ν momentum 75% of the time. The resolution of $|\vec{p}_\nu|$ was about 120 MeV.

The previous CLEO analysis of this decay [11] superseded by this study did not use ν reconstruction. Instead it

TABLE I. Requirements on the kinematic variables. Here, θ is the polar angle between the e^+e^- axis and the momentum of the particle candidate. The γ in E_γ is a daughter of a π^0 candidate.

Variables	Requirements
$ \vec{p}_{\pi^+} $	$> 0.5 \text{ GeV}/c$
$ \vec{p}_{K^-} $	$> 0.5 \text{ GeV}/c$
$ \vec{p}_{\pi^0} $	$> 0.18 \text{ GeV}/c$
$ \vec{p}_e $	$> 0.7 \text{ GeV}/c$ for $ \cos\theta \leq 0.81$
$ \vec{p}_\mu $	$> 1.4 \text{ GeV}/c$ for $ \cos\theta \leq 0.61$
$ \vec{p}_\mu $	$> 1.9 \text{ GeV}/c$ for $0.61 < \cos\theta \leq 0.81$
E_γ	$\geq 30 \text{ MeV}$ for $ \cos\theta < 0.61$
E_γ	$\geq 50 \text{ MeV}$ for $ \cos\theta \geq 0.61$
$ \vec{p}_{K\pi l} $	$> 2.0 \text{ GeV}/c$
$m_{K\pi l}$	$1.2\text{--}1.8 \text{ GeV}/c^2$
$ \vec{p}_{K\pi} $	$> 0.7 \text{ GeV}/c$

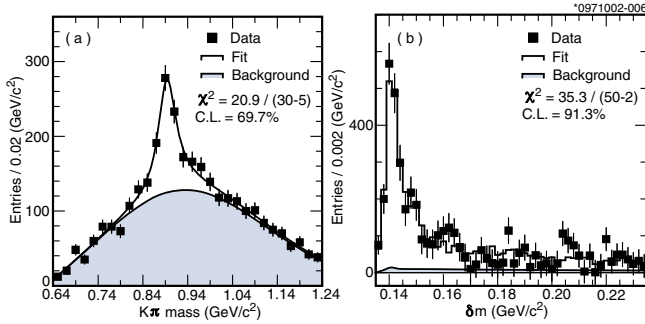


FIG. 1 (color online). The distributions of (a) $K\pi$ mass in the third δm bin and (b) δm for the $D^+ \rightarrow \bar{K}^{*0} e^+ \nu_e$ analysis using 8.78 fb^{-1} data. Points are data. The solid lines are the results of our fits, which include both signal and background, and the shaded areas represent our background estimate.

used the pseudo mass difference, $\delta m_p = m_{K\pi l \pi^0} - m_{K\pi l}$, and the resolution of δm_p was much inferior to δm . The ν reconstruction reduced the statistical uncertainty in the $\mathcal{B}(D^+ \rightarrow \bar{K}^{*0} l^+ \nu_l)$ measurement by 20% according to studies using signal and generic continuum Monte Carlo (MC) events based on our understanding of the electron annihilations into hadrons: $e^+ e^- \rightarrow q\bar{q}$. However, since our method for choosing among the three solutions for $|\vec{p}_\nu|$ tends to bias the δm distribution of the background toward the signal region, it is important to understand the contribution of the background that peaks in the signal region. The uncertainty coming from this effect was included in the systematic errors.

Two quantities were fitted to obtain the number of signal events: $m_{K\pi}$ and δm . First, the data were divided into 50 bins (25 bins for the smaller muon data sample) over the δm range from 0.135 to 0.235 GeV/c^2 . For each δm bin, the $K\pi$ mass distribution was plotted and the number of K^* was extracted by a fit. Second, these yields were plotted as a function of δm , and the number of signal events was obtained by another fit. In the $K\pi$ mass fit, the signal shape was described by a p -wave Breit-Wigner distribution. The mass and width of K^* obtained by the fit were consistent with the Particle Data Group (PDG) values [10]. An analytic threshold function,

$$(m_{K\pi} - 0.63)^\alpha e^{\beta(m_{K\pi} - 0.63) + \gamma(m_{K\pi} - 0.63)^2}, \quad (1)$$

parametrized the shape of the background. The appropriateness of this function was tested using generic continuum MC events after discarding the signal among those events. The parameters α , β , and γ in this background function were unconstrained in the data fits. A typical $K\pi$ mass fit in the δm signal region is shown in Fig. 1(a).

We used the δm distribution of the signal MC sample to describe the signal shapes in the δm fits, whereas a continuous function, which was designed to accommodate the excess at $m_{D^{*+}} - m_{D^+}$ due to our neutrino momentum selection method, was used to represent the

TABLE II. The fractional systematic errors of R from various sources for electron, muon, and electron-muon (l) combined results in units of 10^{-2} .

Source	e	μ	l
Fits			
δm signal shape	2.2	3.3	1.9
δm background shape	1.2	1.4	1.0
Data MC difference (signal)	0.34	0.95	0.32
Data MC difference (background)	2.6	2.5	2.6
Lepton id	1.1	0.27	0.89
Fake leptons	0.064	0.95	0.17
Signal MC model dependence	0.74	0.72	0.73
Efficiency by fragmentation	0.53	0.54	0.53
Feed down	0.18	0.17	0.18
$D^+ \rightarrow \bar{K}^{*0} \pi^0 l^+ \nu_l$	2.6	2.5	2.6
Normalization mode			
Signal shape	1.1	1.1	1.1
Background shape	0.81	0.79	0.81
TOTAL	4.8	6.0	4.7

background shape. The values of this function parameters determining the background shape were obtained by a fit to the background distribution attained from a generic continuum MC sample. These values of the parameters were fixed in the fit to data. The overall efficiencies in the electron and muon mode analyses were found to be 5.5% and 0.9%, respectively. The δm fit of the electron data is shown in Fig. 1(b).

The decay chain, $D^{*+} \rightarrow D^+ \pi^0$, $D^+ \rightarrow K^- \pi^+ \pi^+$, was used for the normalization mode. One advantage of this mode is that many systematic errors in its “measurement” are common with the $D^+ \rightarrow \bar{K}^{*0} l^+ \nu$ mode and cancel in their ratio. Furthermore, the branching fraction of $D^+ \rightarrow K^- \pi^+ \pi^+$ is well measured: $(9.0 \pm 0.6)\%$ [10]. Most of the kinematic requirements were the same as those in the semileptonic analysis. The requirement on the momentum of the D^* candidates was equivalent to the requirement on $|\vec{p}_{K\pi l}|$ for our signal semileptonic mode

TABLE III. Results of the R_e^+ , R_μ^+ , and R_l^+ measurements and the branching fractions \mathcal{B}_e , \mathcal{B}_μ , and \mathcal{B}_l (see text). The first and second errors in the R and \mathcal{B} measurements are due to statistical and systematic errors, respectively. The third errors in the \mathcal{B} measurements are due to the uncertainty in $\mathcal{B}(D^+ \rightarrow K^- \pi^+ \pi^+)$.

R_e^+	$0.74 \pm 0.04 \pm 0.05$
R_μ^+	$0.72 \pm 0.10 \pm 0.05$
R_l^+	$0.74 \pm 0.04 \pm 0.05$
\mathcal{B}_e	$(6.7 \pm 0.4 \pm 0.5 \pm 0.4)\%$
\mathcal{B}_μ	$(6.5 \pm 0.9 \pm 0.5 \pm 0.4)\%$
\mathcal{B}_l	$(6.7 \pm 0.4 \pm 0.5 \pm 0.4)\%$

TABLE IV. Comparison of the measured values of R_e^+ and R_μ^+ .

Group	R_e^+	Group	R_μ^+
CLEO (2001)	$0.74 \pm 0.04 \pm 0.05$	CLEO (2001)	$0.72 \pm 0.10 \pm 0.05$
PDG [10]	0.54 ± 0.05	PDG [10]	0.53 ± 0.06
CLEO [11]	$0.67 \pm 0.09 \pm 0.07$	E687 [12]	$0.56 \pm 0.04 \pm 0.06$
OMEG [13]	$0.62 \pm 0.15 \pm 0.09$	E653 [16]	$0.46 \pm 0.07 \pm 0.08$
ARGUS [14]	$0.55 \pm 0.08 \pm 0.10$		
E691 [15]	$0.49 \pm 0.04 \pm 0.05$		

to minimize our sensitivity to the uncertainty in the fragmentation of the charm quarks.

For the normalization mode analysis, two successive fits of m_{D^+} and δm were used. The data were divided into 50 δm bins from 0.135 to 0.185 GeV/ c^2 . For each δm bin, a D^+ mass fit was used to extract the number of D^+ . These yields of D^+ were plotted as a function of δm . Then, this δm plot was fitted to obtain the number of the normalization mode events. The calculated efficiency in the normalization mode analysis was 6.3%.

Table II lists the important contributions to the systematic error. The dominant sources are the δm signal shape estimation due to finite MC statistics, potential flaws in the estimate of the background shape obtained from the simulation of $e^+e^- \rightarrow q\bar{q}$, and background arising from $D^+ \rightarrow \bar{K}^{*0}\pi^0 l^+ \nu_l$. Reference [9] contains a detailed discussion of the systematic errors and their derivations.

The ratio R_l^+ was calculated using

$$R_l^+ = \frac{N_{sl}}{\epsilon_{sl} \mathcal{B}(\bar{K}^{*0} \rightarrow K^- \pi^+)} \frac{\epsilon_{had}}{N_{had}}, \quad (2)$$

where N_{sl} and ϵ_{sl} are the observed number of events and the efficiency for $D^+ \rightarrow \bar{K}^{*0} l^+ \nu_l$, respectively. Similarly, N_{had} and ϵ_{had} are the corresponding quantities for $D^+ \rightarrow K^- \pi^+ \pi^+$. The measured branching ratios R_e^+ , R_μ^+ , and R_l^+ , including their errors, are summarized in Table III. The values of R_e^+ and R_μ^+ agree well. The PDG value of $\mathcal{B}(D^+ \rightarrow K^- \pi^+ \pi^+) = (9.0 \pm 0.6)\%$ [10] was used to calculate the branching fractions of $D^+ \rightarrow \bar{K}^{*0} e^+ \nu_e$ (\mathcal{B}_e), $D^+ \rightarrow \bar{K}^{*0} \mu^+ \nu_\mu$ (\mathcal{B}_μ), and $D^+ \rightarrow \bar{K}^{*0} l^+ \nu_l$ (\mathcal{B}_l). Our analysis results were checked using nine different analysis methods as described in other literature [9], and all methods provided the consistent results within errors.

Table IV compares the results of this work with previous measurements [11–16] and the PDG averages [10]. Note that the E691 measurement of R_e^+ and ours are the two most significant measurements, and they differ by about three standard deviations. We studied whether this difference (or part thereof) may arise from differences between the $D^+ \rightarrow \bar{K}^{*0} e^+ \nu_e$ model used here (ISGW2) [17] and the one used in the E691 analysis (WSB) [18]. Since the lepton momentum distribution expected from this decay has a significant effect on its detection efficiency in both experiments, we compared the electron

energy and q^2 distributions from the two models, but found no significant differences. We did not identify any other explanations for the discrepancy. This discrepancy calls into question about the accuracy of the form factors obtained using the E691 branching fraction measurements.

Table V shows the decay rate for $D^+ \rightarrow \bar{K}^{*0} e^+ \nu_e$ measured in this work and the theoretical predictions [17,19–23]. Most predictions are consistent with both our result and that of E691. Using our branching ratio measurements and the ratios between the form factors measured by E791 [24], we calculate $A_1(0) = 0.69 \pm 0.06$, $A_2(0) = 0.50 \pm 0.07$, and $V(0) = 1.26 \pm 0.14$, where the errors are the quadratic sums of the statistical and systematic errors in this analysis and in the E791 measurement.

The ratio of the vector and pseudoscalar decay widths, $r_{vp} = [\Gamma(D \rightarrow K^* e^+ \nu_e)]/[\Gamma(D \rightarrow K e^+ \nu_e)]$, tests quark models. This ratio was predicted to be in the range 0.9 to 1.2 by early quark models [18,25–28] and lattice gauge calculations [29,30]. The E691 result implied that $r_{vp} = 0.48 \pm 0.10$. The newer ISGW2 model [17] accommodated this measurement well, predicting $r_{vp} = 0.54$. Our measurement of R_l^+ , on the other hand, implies that $r_{vp} = 0.99 \pm 0.06 \pm 0.07 \pm 0.06$, where the first, second, and third errors are due to our statistical and systematic errors and the uncertainty in $\mathcal{B}(D^+ \rightarrow \bar{K}^{*0} e^+ \nu_e)$, respectively, using the PDG value of $\mathcal{B}(D^+ \rightarrow \bar{K}^{*0} e^+ \nu_e) = (6.8 \pm 0.8)\%$ [10]. Our ratio is consistent with older

TABLE V. Comparison of the decay rate for $D^+ \rightarrow \bar{K}^{*0} e^+ \nu_e$ measured in this work with those theoretically predicted and the present PDG value. All values are in units of $10^{10}|V_{cs}|^2 \text{ sec}^{-1}$.

Group	Decay rate ($10^{10} V_{cs} ^2 \text{ sec}^{-1}$)
CLEO (2001)	6.62 ± 0.74
PDG [10]	4.79 ± 0.40
UKQCD (2001) [19]	5.8 ± 0.5
APE [20]	7.3 ± 1.9
UKQCD (1994) [21]	$6.3^{+0.8}_{-1.7}$
ELC [22]	6.7 ± 2.9
LMMS [23]	5.3 ± 0.9
ISGW2 [17]	5.7

models and disagrees with the ISGW2 prediction by four standard deviations.

Based on the result of this work, we can conclude three things. First, our R_e^+ is about three standard deviations larger than the R_e^+ of E691, which is the dominant measurement in the PDG average. Second, the $D^+ \rightarrow \bar{K}^{*0} e^+ \nu_e$ decay rate measured in this work consists with the lattice gauge calculations and ISGW2 model prediction. In the third, our r_{vp} is consistent with the predictions of quark models but the ISGW2 model. Our r_{vp} is larger than the ISGW2 model prediction by four standard deviations.

We gratefully acknowledge the effort of the CESR staff in providing us with excellent luminosity and running conditions. This work was supported by the National Science Foundation, the U.S. Department of Energy, the Research Corporation, the Natural Sciences and Engineering Research Council of Canada, and the Texas Advanced Research Program.

-
- [1] B. Stech, in *Proceedings of the Fifth Moriond Workshop, Flavor Mixing and CP-Violation*, edited by J. Tran Thanh Van (La Plagne, France, 1985), p. 151.
- [2] N. Isgur and M. B. Wise, Phys. Lett. B **232**, 113 (1989); N. Isgur and M. B. Wise, Phys. Lett. B **237**, 527 (1990).
- [3] E. Eichten and B. Hill, Phys. Lett. B **243**, 427 (1990); H. Georgi, Phys. Lett. B **240**, 447 (1990).
- [4] M. Neubert, Phys. Rep. **245**, 259 (1994).
- [5] M. Adamovich *et al.*, Eur. Phys. J. C **6**, 35 (1999), and references therein.
- [6] Y. Kubota *et al.*, Nucl. Instrum. Methods Phys. Res., Sect. A **320**, 66 (1992); T. Hill *et al.*, Nucl. Instrum. Methods Phys. Res., Sect. A **418**, 32 (1998).
- [7] S. Brandt *et al.*, Phys. Lett. **12**, 57 (1964); E. Farhi, Phys. Rev. Lett. **39**, 1587 (1977).
- [8] G.C. Fox and S. Wolfram, Phys. Rev. Lett. **41**, 1581 (1978).
- [9] S.J. Lee, Ph.D. thesis, University of Minnesota, 2001.
- [10] S.J. Lee, Particle Data Group, Eur. Phys. J. C **15**, 1 (2000).
- [11] A. Bean *et al.*, Phys. Lett. B **317**, 647 (1993).
- [12] P.L. Frabetti *et al.*, Phys. Lett. B **307**, 262 (1993).
- [13] M. Adamovich *et al.*, Phys. Lett. B **268**, 142 (1991).
- [14] H. Albrecht *et al.*, Phys. Lett. B **255**, 634 (1991).
- [15] J.C. Anjos *et al.*, Phys. Rev. Lett. **62**, 722 (1989).
- [16] K. Kodama *et al.*, Phys. Lett. B **286**, 187 (1992).
- [17] D. Scora and N. Isgur, Phys. Rev. D **52**, 2783 (1995).
- [18] M. Wirbel, B. Stech, and M. Bauer, Z. Phys. C **29**, 637 (1985).
- [19] J. Gill *et al.*, hep-lat/0109035.
- [20] C.R. Allton, Phys. Lett. B **345**, 513 (1995).
- [21] K. Bowler *et al.*, Phys. Rev. D **51**, 4905 (1995).
- [22] A. Abada *et al.*, Nucl. Phys. B **416**, 675 (1994).
- [23] V. Lubicz, G. Martinelli, M. McCarthy, and C.T. Sachrajda, Phys. Lett. B **274**, 415 (1992).
- [24] E.M. Aitala *et al.*, Phys. Lett. B **440**, 435 (1998).
- [25] T. Altomari and L. Wolfenstein, Phys. Rev. D **37**, 681 (1988).
- [26] J.G. Korner and G.A. Schuler, Z. Phys. C **38**, 511 (1988).
- [27] N. Isgur, D. Scora, B. Grinstein, and M.B. Wise, Phys. Rev. D **39**, 799 (1989).
- [28] F.J. Gilman and R.L. Singleton, Phys. Rev. D **41**, 142 (1990).
- [29] C.W. Bernard, A.X. El-Khadra, and A. Soni, Phys. Rev. D **43**, 2140 (1991); C.W. Bernard, A.X. El-Khadra, and A. Soni, Phys. Rev. D **45**, 869 (1992); C.W. Bernard, A.X. El-Khadra, and A. Soni, Phys. Rev. D **47**, 998 (1993).
- [30] V. Lubicz, G. Martinelli, M.S. McCarthy, and C.T. Sachrajda, Phys. Lett. B **274**, 415 (1992).